Shocks and cosmic ray acceleration in MHD simulations

Christoph Pfrommer[1]

in collaboration with

PhD students: K. Ehlert,[1] L. Jlassi,[1] R. Lemmerz,[1]
J. Whittingham,[1] M. Weber[1]
T. Berlok,[1] V. Bresci,[1] P. Girichidis,[2] M. Pais,[3] K. Schaal, R. Pakmor,[4]
L. Perrone,[1] M. Shalaby,[1] C. Simpson,[5] M. Sparre,[6,1] V. Springel,[4]
T. Thomas,[1] M. Werhahn[1], G. Winner

[1]AIP Potsdam, [2]U of Heidelberg, [3]Hebrew U, [4]MPA Garching, [5]U of Chicago, [6]U of Potsdam

Potsdam Plasma Workshop, AIP, Nov 2022

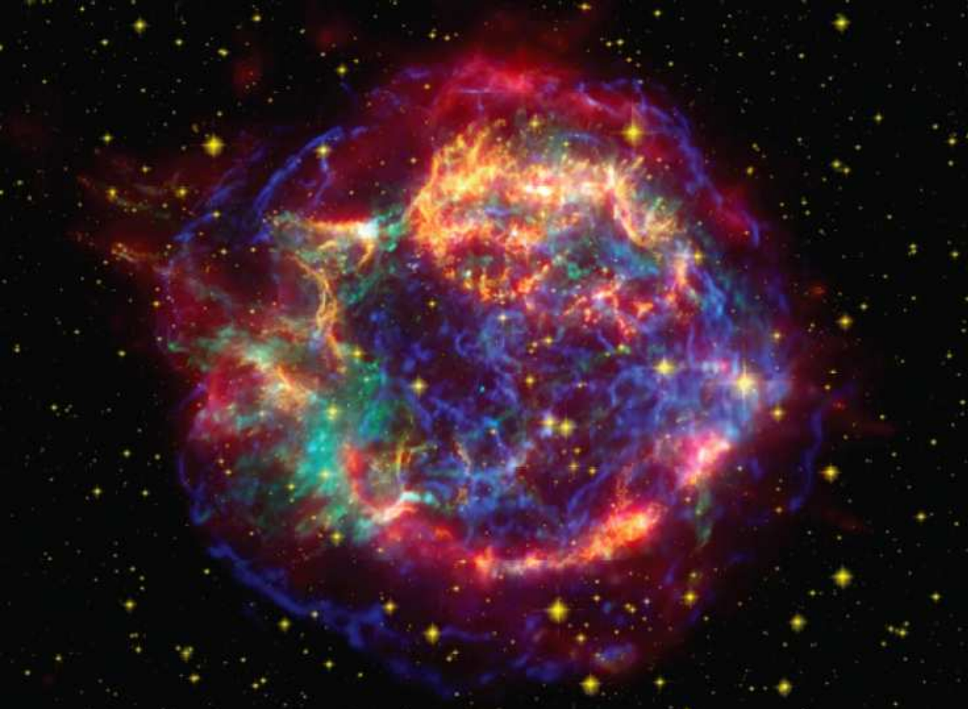

Astrophysical shocks

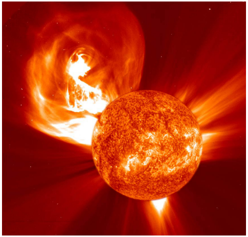

solar system shocks $\sim R_\odot$
coronal mass ejection (SOHO)

interstellar shocks ~ 20 pc
supernova 1006 (CXC/Hughes)

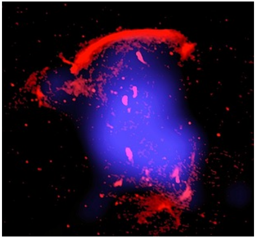

cluster shocks ~ 2 Mpc
giant radio relic (van Weeren)

Astrophysical shocks

Astrophysical collisionless shocks can:

- accelerate particles (electrons and ions) $\rightarrow$ cosmic rays (CRs)
- amplify magnetic fields (or generate them from scratch)

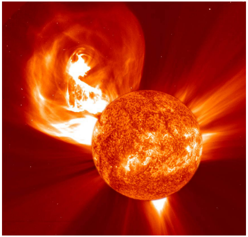

solar system shocks $\sim R_\odot$
coronal mass ejection (SOHO)

interstellar shocks $\sim$ 20 pc
supernova 1006 (CXC/Hughes)

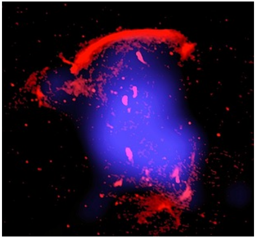

cluster shocks $\sim$ 2 Mpc
giant radio relic (van Weeren)

Astrophysical shocks

Astrophysical collisionless shocks can:

- accelerate particles (electrons and ions) $\rightarrow$ cosmic rays (CRs)
- amplify magnetic fields (or generate them from scratch)

$\Rightarrow$ non-thermal emission (radio to gamma rays)

$\Rightarrow$ cosmic ray feedback in galaxies and galaxy clusters

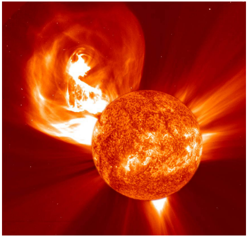

solar system shocks $\sim R_\odot$
coronal mass ejection (SOHO)

interstellar shocks $\sim$ 20 pc
supernova 1006 (CXC/Hughes)

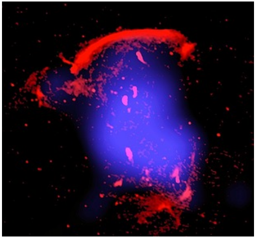

cluster shocks $\sim$ 2 Mpc
giant radio relic (van Weeren)

Unstructured moving-mesh code AREPO (Springel 2010)

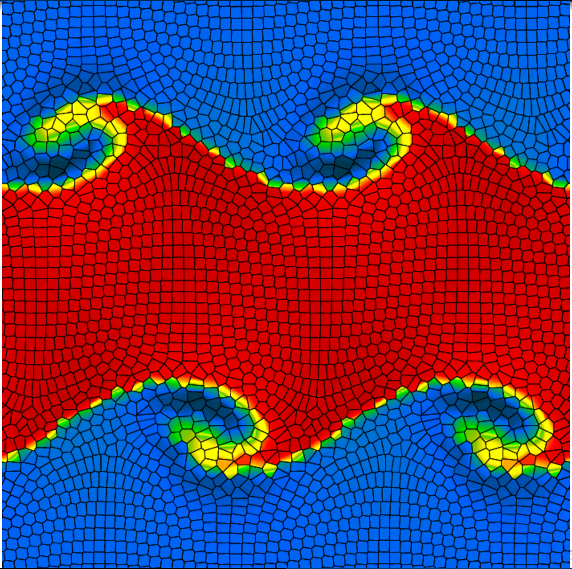

Shock finder

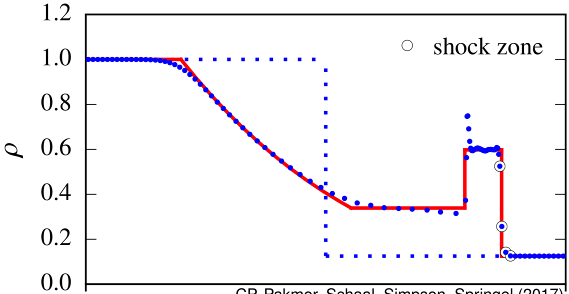

CP, Pakmor, Schaal, Simpson, Springel (2017)

Shock finder

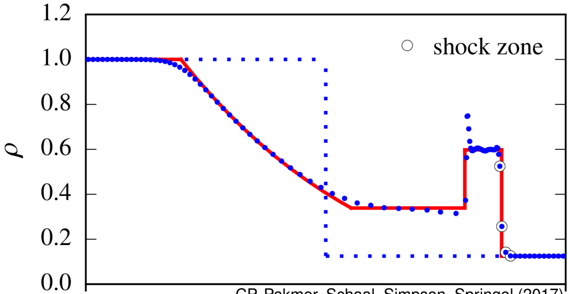

CP, Pakmor, Schaal, Simpson, Springel (2017)

Voronoi cells belong to **shock zone** if

- $\nabla \cdot \boldsymbol{v} < 0$ (converging flow)
- $\nabla T \cdot \nabla \rho > 0$ (filtering out tangential discontinuities)
- $\mathcal{M}_1 > \mathcal{M}_{\min}$ (safeguard against numerical noise)

Shock finder and CR acceleration

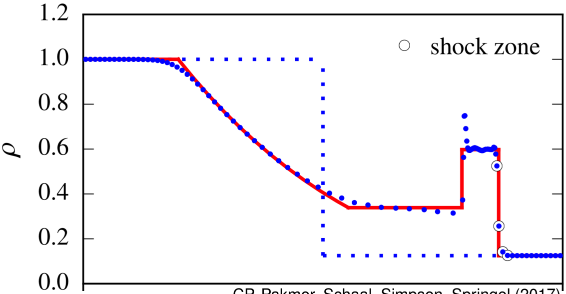

CP, Pakmor, Schaal, Simpson, Springel (2017)

CR acceleration:

- **shock surface:** cell with most converging flow

Shock finder and CR acceleration

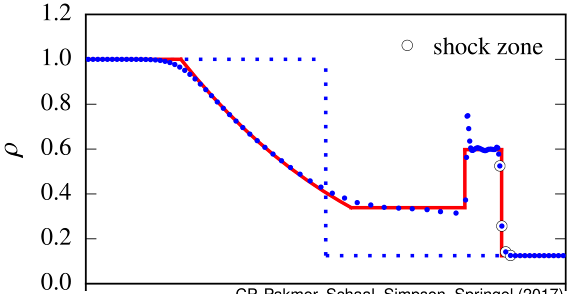

CP, Pakmor, Schaal, Simpson, Springel (2017)

CR acceleration:

- **shock surface:** cell with most converging flow
- collect pre- and post-shock energy at shock surface $\Rightarrow E_{\mathrm{diss}}$
- inject $\Delta E_{\mathrm{cr}} = \zeta(\mathcal{M}_1, \theta)\, E_{\mathrm{diss}}$ to shock and 1st post-shock cell

Shock finder and CR acceleration

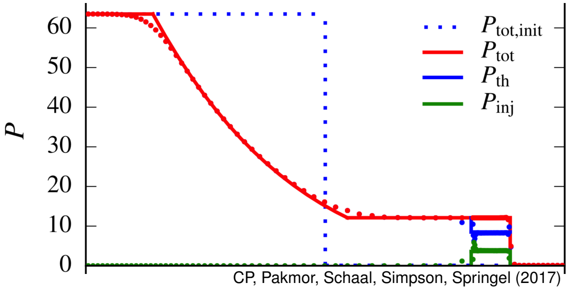

CR acceleration:

- **shock surface:** cell with most converging flow
- collect pre- and post-shock energy at shock surface $\Rightarrow E_{\rm diss}$
- inject $\Delta E_{\rm cr} = \zeta(\mathcal{M}_1, \theta)\, E_{\rm diss}$ to shock and 1[st] post-shock cell

Shock finder and CR acceleration

Comparing simulations to exact solutions that include CR acceleration

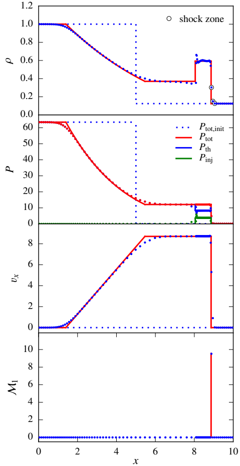

CP, Pakmor, Schaal, Simpson, Springel (2017)

Shock finder and CR acceleration

Comparing simulations to exact solutions that include CR acceleration

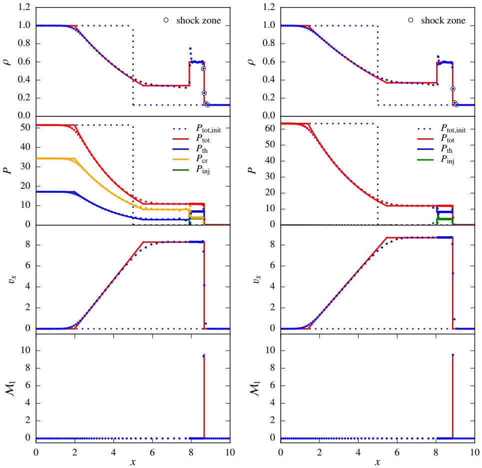

CP, Pakmor, Schaal, Simpson, Springel (2017)

Shock finder and CR acceleration

Comparing simulations to exact solutions that include CR acceleration

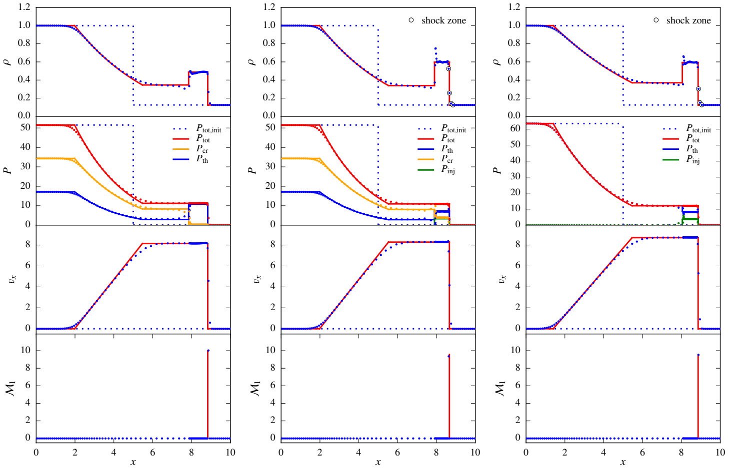

CP, Pakmor, Schaal, Simpson, Springel (2017)

Shock finder and CR acceleration

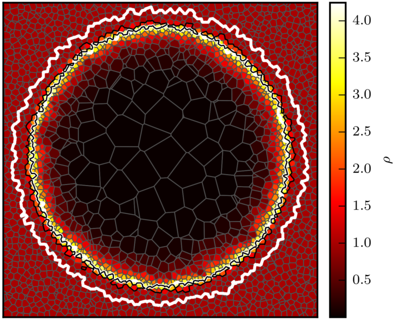

CP, Pakmor, Schaal, Simpson, Springel (2017)

Shock finder and CR acceleration

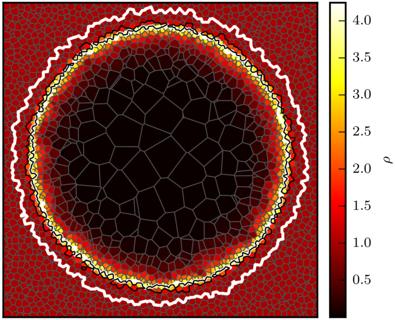

CP, Pakmor, Schaal, Simpson, Springel (2017)

CR acceleration:

- **shock surface:** cell with most converging flow along ∇T

Shock finder and CR acceleration

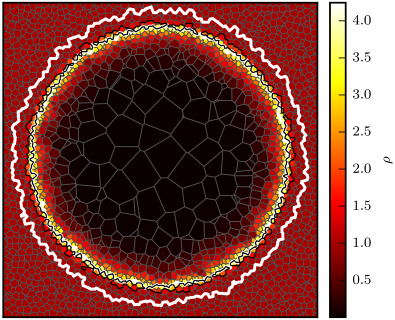

CP, Pakmor, Schaal, Simpson, Springel (2017)

CR acceleration:

- **shock surface:** cell with most converging flow along ∇T
- collect pre- and post-shock energy at shock surface
- inject CR energy to shock and post-shock cell

Shock finder and CR acceleration

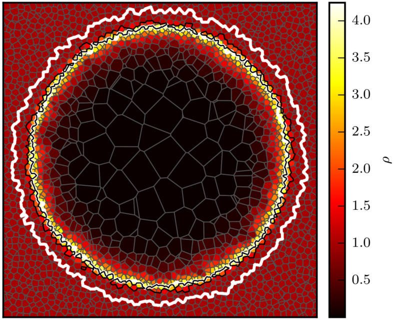

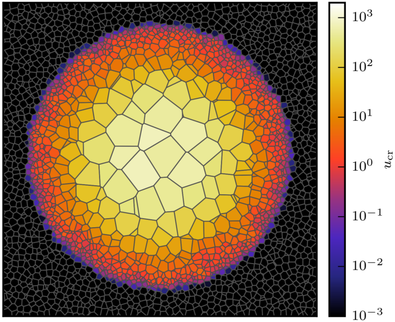

CP, Pakmor, Schaal, Simpson, Springel (2017)

CR acceleration:

- **shock surface:** cell with most converging flow along ∇T
- collect pre- and post-shock energy at shock surface
- inject CR energy to shock and post-shock cell

Sedov explosion

density

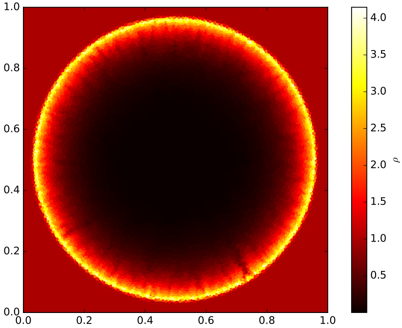

specific thermal energy

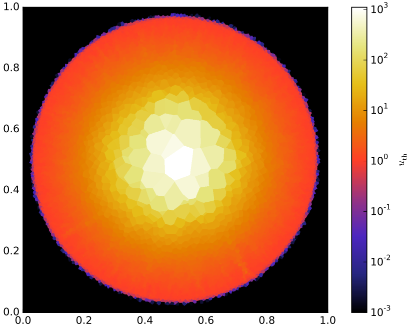

CP, Pakmor, Schaal, Simpson, Springel (2017)

Sedov explosion with CR acceleration

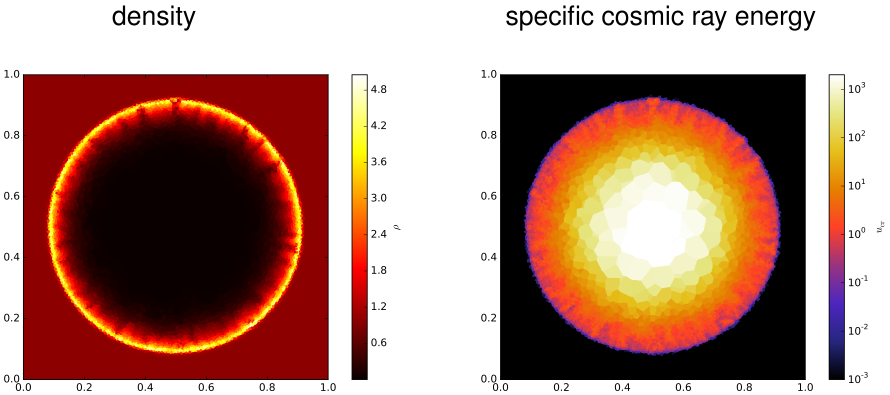

CP, Pakmor, Schaal, Simpson, Springel (2017)

Sedov explosion with CR acceleration

adiabatic index

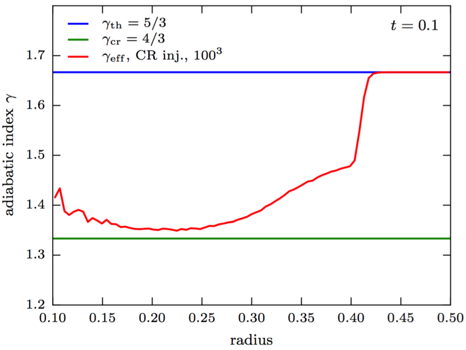

shock evolution

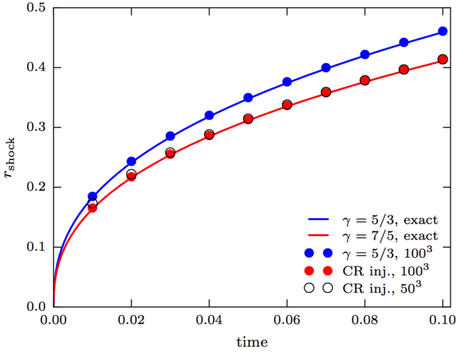

CP, Pakmor, Schaal, Simpson, Springel (2017)

Global MHD simulations of SNRs with CR physics

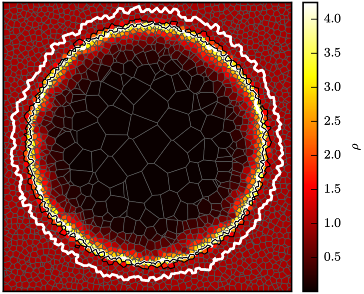

Mach number finder with CRs

CP+ (2017)

- detect and characterize shocks and jump conditions on the fly

Global MHD simulations of SNRs with CR physics

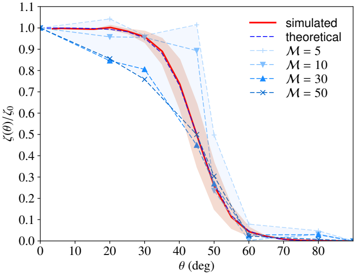

obliquity-dep. acceleration efficiency

Pais, CP+ (2018) based on
hybrid PIC sim.'s by Caprioli & Spitkovsky (2015)

- detect and characterize shocks and jump conditions on the fly
- measure Mach number $\mathcal{M}$ and magnetic obliquity θ_B

Global MHD simulations of SNRs with CR physics

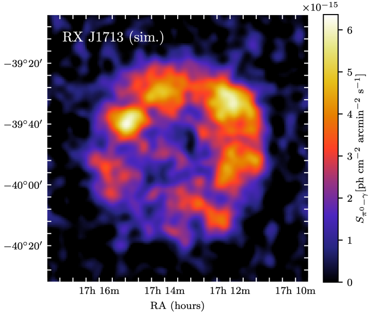

simulated TeV gamma-ray map

Pais & CP (2020)

- detect and characterize shocks and jump conditions on the fly
- measure Mach number $\mathcal{M}$ and magnetic obliquity θ_B
- inject and transport CR protons
  $\Rightarrow$ dynamical back reaction on gas flow, hadronic emission

Global MHD simulations of SNRs with CR physics

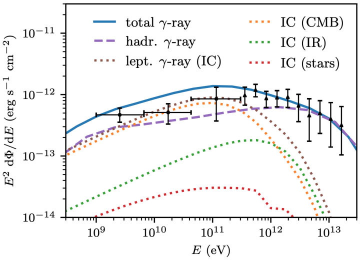

simulated gamma-ray spectrum

Winner, CP+ (2019, 2020)

- detect and characterize shocks and jump conditions on the fly
- measure Mach number $\mathcal{M}$ and magnetic obliquity θ_B
- inject and transport CR protons $\Rightarrow$ dynamical back reaction on gas flow, hadronic emission
- inject and transport CR electrons
- calculate non-thermal radio, X-ray, γ-ray emission

Hadronic TeV γ rays: SN 1006

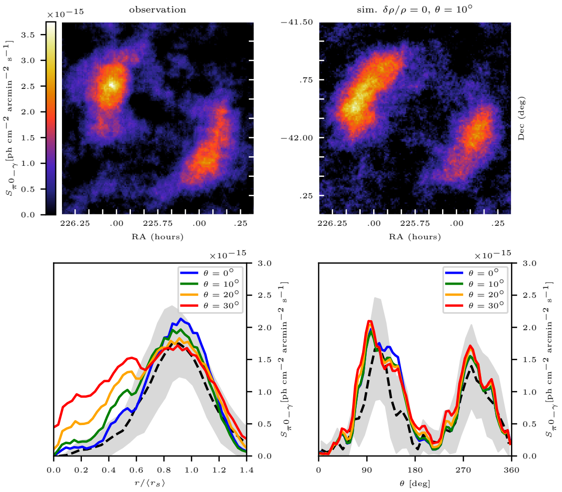

Pais & CP (2020)

Hadronic TeV γ rays: SN 1006

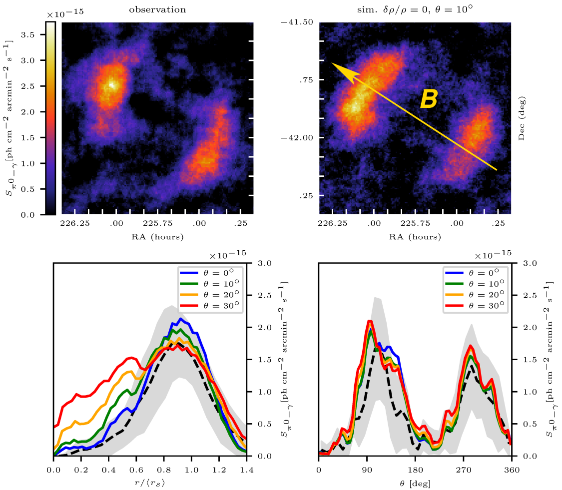

Pais & CP (2020)

Hadronic TeV γ rays: Vela Jr. and RXJ 1713

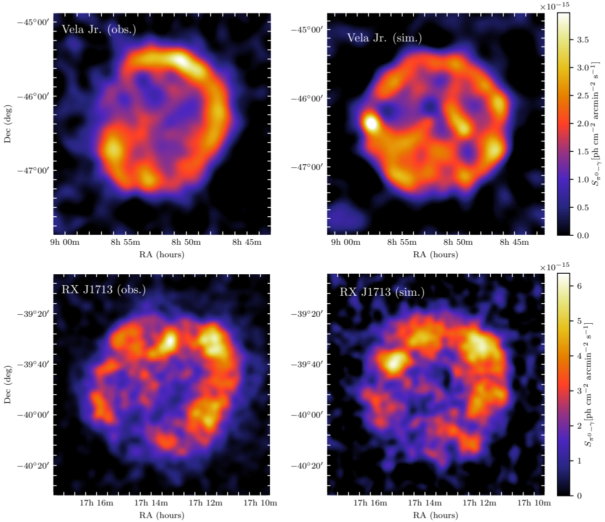

Pais & CP (2020)

TeV γ rays from shell-type supernova remnants

Varying magnetic coherence scale in simulations of SN 1006 and Vela Junior

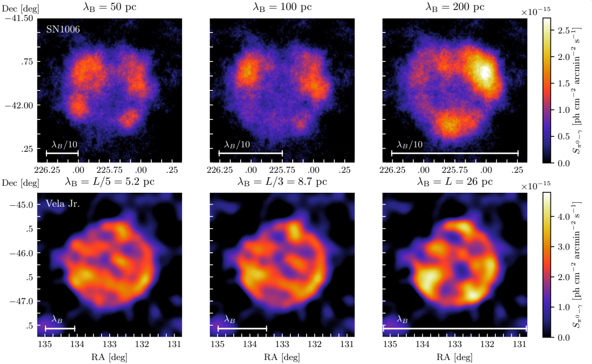

TeV γ rays from shell-type supernova remnants

Varying magnetic coherence scale in simulations of SN 1006 and Vela Junior

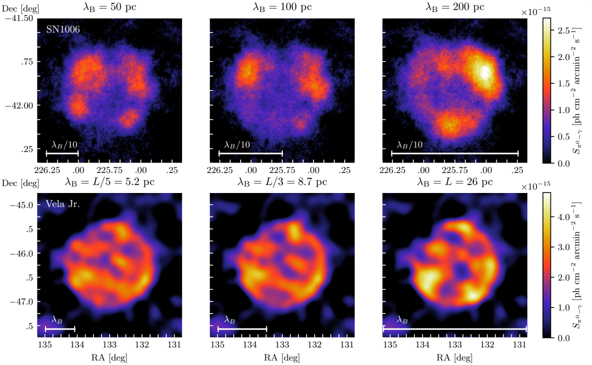

Pais, CP+ (2020)

$\Rightarrow$ Correlation structure of patchy TeV γ-rays constrains magnetic coherence scale in ISM:

SN 1006: $\lambda_B > 200^{+80}_{-10}$ pc   Vela Junior: $\lambda_B = 13^{+13}_{-4.3}$ pc

CREST - Cosmic Ray Electron Spectra evolved in Time

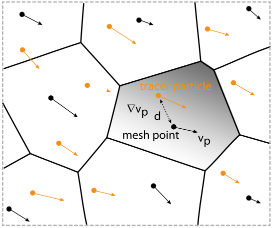

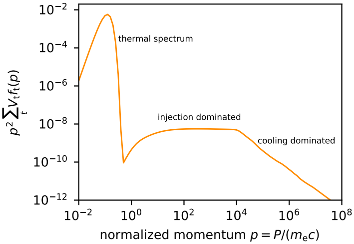

CREST code (Winner, CP+ 2019)

- post-processing MHD simulations
- on Lagrangian particles
  - adiabatic processes
  - Coulomb and radiative losses
  - Fermi-I (re-)acceleration
  - Fermi-II reacceleration
  - secondary electrons

Link to observations

- radio synchrotron
- inverse Compton (IC) γ-ray

AIP

Sedov–Taylor blast wave: spectral evolution

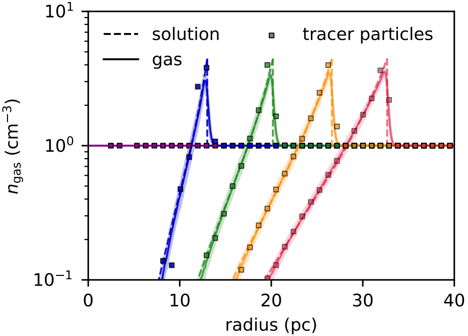

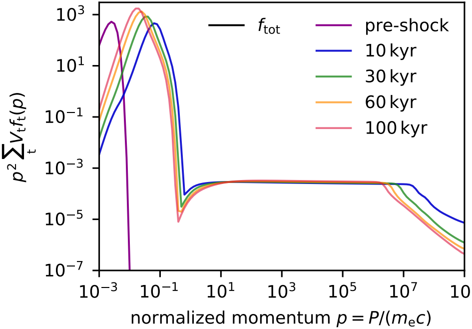

Winner, CP+ (2019)

$$E_0 = 10^{51}\,\mathrm{erg},\ \ n_{\rm gas} = 1\,\mathrm{cm}^{-3},\ \ T_0 = 10^4\,\mathrm{K},\ \ B = 1\,\mu\mathrm{G}$$

SN 1006: CR electron acceleration models

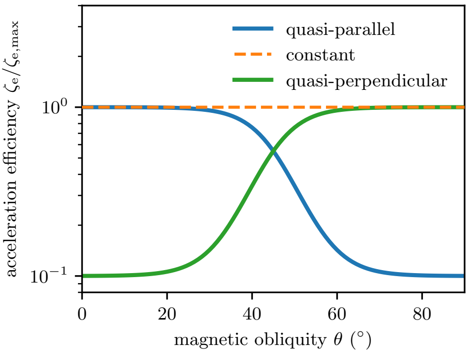

Winner, CP+ (2020)

- different obliquity dependent electron acceleration efficiencies:
  1. preferred quasi-perpendicular acceleration (previous PIC)
  2. constant acceleration efficiency (a straw man's model)
  3. preferred quasi-parallel acceleration (like CR protons)

CR electron acceleration: quasi-perpendicular shocks

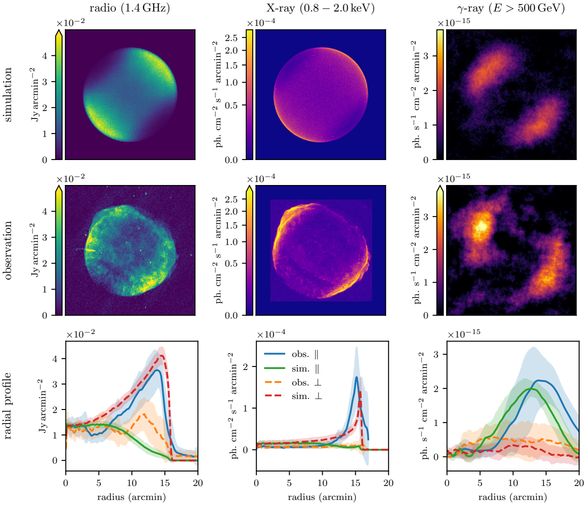

Winner, CP+ (2020)

CR electron acceleration: constant efficiency

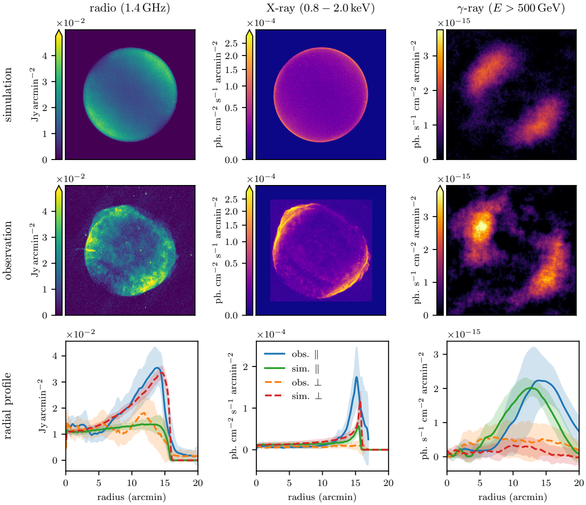

Winner, CP+ (2020)

CR electron acceleration: quasi-parallel shocks

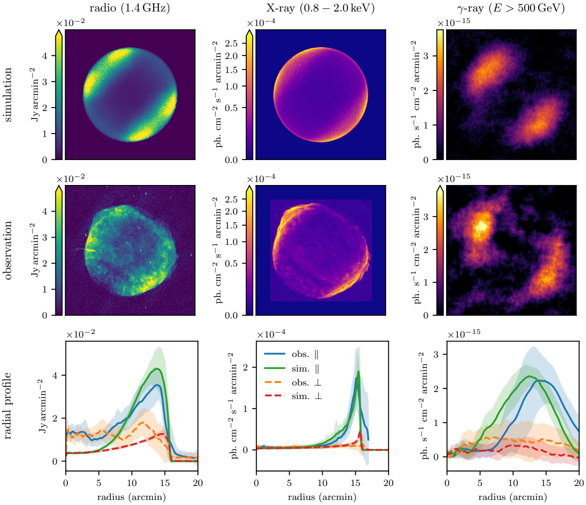

Winner, CP+ (2020)

SN 1006: multi-frequency spectrum

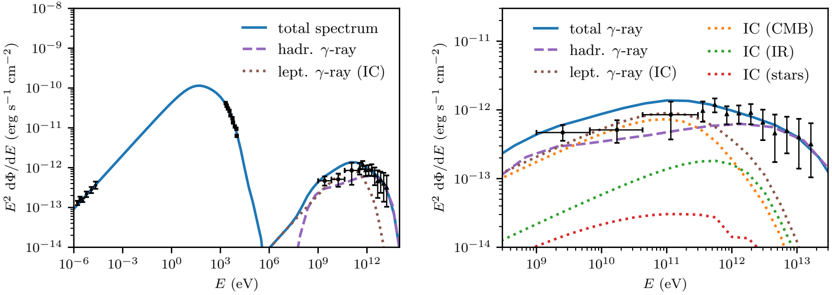

Winner, CP+ (2020)

- quasi-parallel acceleration model fits multi-frequency spectrum

SN 1006: multi-frequency spectrum

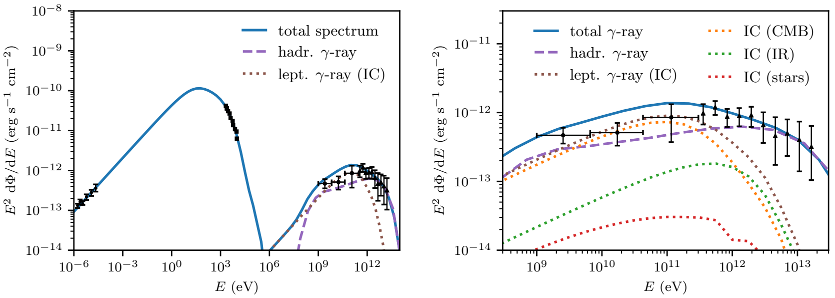

Winner, CP+ (2020)

- quasi-parallel acceleration model fits multi-frequency spectrum
- GeV regime: leptonic inverse Compton dominates
- TeV regime: hadronic pion decay

SN 1006: maps of γ-ray components at $E > 500$ GeV

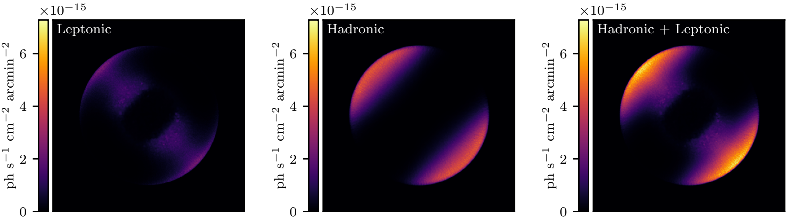

Winner, CP+ (2020)

- hadronic pion decay emission dominant at shock rim
- leptonic IC emission has contributions from SNR interior

SN 1006: magnetic field amplification models

Magnetic amplification due to a turbulent dynamo and Bell's instability

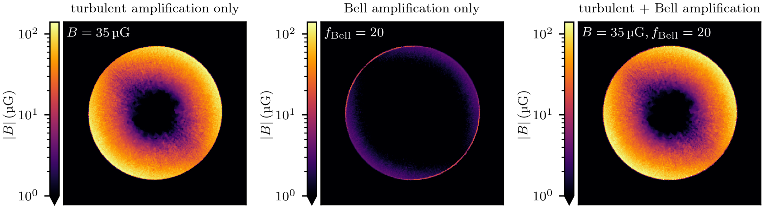

Winner, CP+ (2020)

- magnetic field strength in a slice through the simulated SNRs

SN 1006: magnetic field amplification models

Magnetic amplification due to a turbulent dynamo and Bell's instability

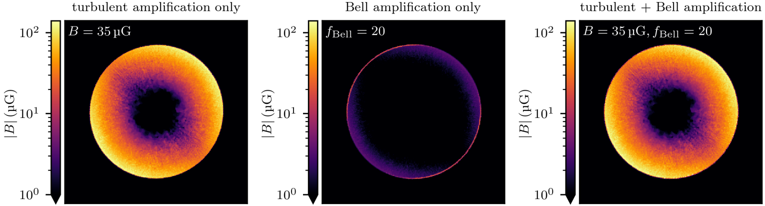

Winner, CP+ (2020)

- magnetic field strength in a slice through the simulated SNRs
- left: effect of turbulent amplification only, maximum realized at quasi-perpendicular shock, adiabatic cooling inside the SNR
- middle: effect of Bell amplification only, f_{Bell} follows obliquity dependence of CR proton efficiency
- right: sum of both, turbulent and Bell amplification

Constraining the volume-filling, turbulent *B* field

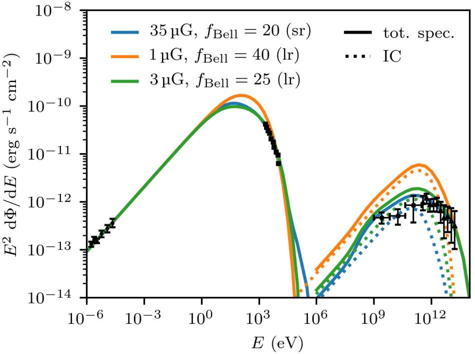

Winner, CP+ (2020)

- multi-frequency spectra: synchrotron (radio + X-rays) and IC and hadronic γ-ray emission

Constraining the volume-filling, turbulent *B* field

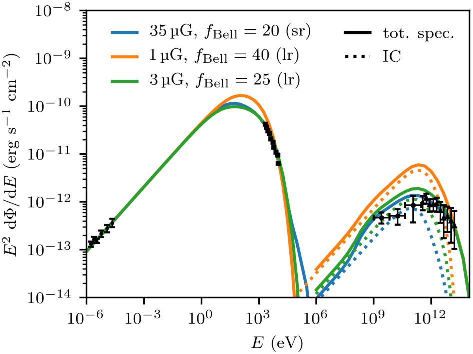

Winner, CP+ (2020)

- multi-frequency spectra: synchrotron (radio + X-rays) and IC and hadronic γ-ray emission
- strong, volume-filling ***B*** field ($\approx$ 35 μG) required to suppress IC γ-ray component and to match steep X-ray spectrum

SN 1006: best-fit multi-frequency spectrum

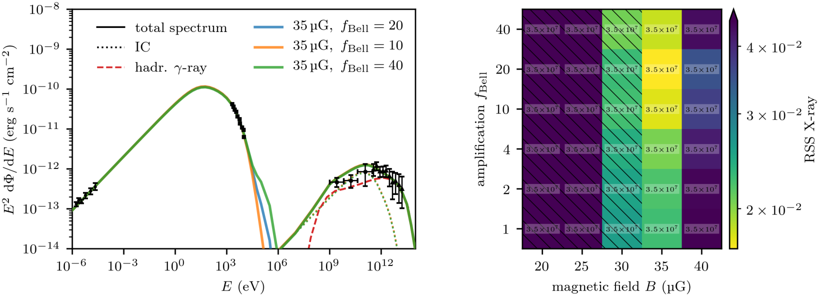

Winner, CP+ (2020)

- parameter optimization of magnetic amplification processes

SN 1006: best-fit multi-frequency spectrum

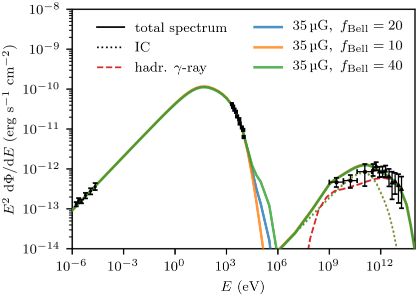

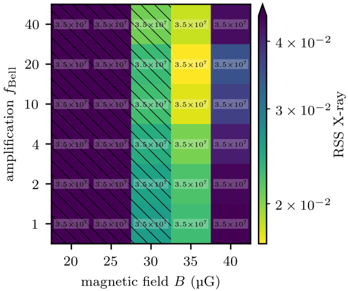

Winner, CP+ (2020)

- parameter optimization of magnetic amplification processes
- strong ($\approx$ 35 μG) volume-filling ***B*** field (turbulent dynamo): lower *B* field excluded by IC component
- Bell-amplification factor $f_{\rm Bell}$ 10 – 20 weakly constrained

Conclusions for CR hydrodynamics at SNRs

CR hydrodynamics with kinetic plasma physics:

- Shock finder enables CR acceleration in MHD simulations
- CR proton transport in MHD enables dynamic backreaction
- CR electron spectral transport (CREST): multi-frequency spectra and emission maps

Conclusions for CR hydrodynamics at SNRs

CR hydrodynamics with kinetic plasma physics:

- Shock finder enables CR acceleration in MHD simulations
- CR proton transport in MHD enables dynamic backreaction
- CR electron spectral transport (CREST): multi-frequency spectra and emission maps

CR acceleration constraints by MHD models:

- TeV shell-type SNRs probe magnetic coherence scale in ISM
- hybrid-PIC simulations of p^+ acceleration agree with global SNR simulations
- global SNR simulations imply preferred quasi-parallel e^- acceleration: new intermediate instability enables e^- (pre-)acceleration

PICOGAL: From Plasma KInetics to COsmological GALaxy Formation

This project has received funding from the European Research Counsil (ERC) under the European Union's Horizon 2020 research and innovation program (grant agreement No PICOGAL–101019746).

Literature for the talk

Cosmic ray hydrodynamics and shock acceleration:

- Pfrommer, Pakmor, Schaal, Simpson, Springel, *Simulating cosmic ray physics on a moving mesh* 2017, MNRAS, 465, 4500.

Cosmic ray electron spectra in MHD:

- Winner, Pfrommer, Girichidis, Pakmor, *Evolution of cosmic ray electron spectra in magnetohydrodynamical simulations,* 2019, MNRAS, 488, 2235.
- Winner, Pfrommer, Girichidis, Werhahn, Pais, *Evolution and observational signatures of the cosmic ray electron spectrum in SN 1006,* 2020, MNRAS, 499, 2785.

Cosmic ray proton acceleration at SNRs:

- Pais, Pfrommer, Ehlert, Pakmor, *The effect of cosmic-ray acceleration on supernova blast wave dynamics,* 2018, MNRAS, 478, 5278.
- Pais, Pfrommer, Ehlert, Werhahn, Winner, *Constraining the coherence scale of the interstellar magnetic field using TeV gamma-ray observations of supernova remnants,* 2020, MNRAS, 496, 2448.
- Pais, Pfrommer, *Simulating TeV gamma-ray morphologies of shell-type supernova remnants,* 2020, MNRAS, 498, 5557.